Interactive Software for Rendering Electromagnetic Fields:

Structures and Algorithms

DSBirkett
Wentworth Institute April 4, 2016

1. Lines of force and equipotential surfaces.

Since Maxwell and Faraday, graphical techniques have been employed to illustrate the properties of the electromagnetic field. In a series of fine plates at the end of Maxwell's treatise of 1873 electrostatic field lines and equipotential surfaces are accurately displayed in a variety of geometries. The steady advance of computing technology, using a wide variety of mathematical methods, has made the depiction of electromagnetic fields ever easier. Notable among these methods is finite element analysis (FEA), probably the most powerful general approach, though even FEA is of limited applicability in many geometries.

In exposition of the properties of the electromagnetic field, it is highly desirable that an interactive interface be employed. With such an interface an operator can specify and then modify a given geometry incrementally to examine how the field changes in response. This requires that the interface be sufficiently fast that the field lines can be rendered in a few seconds or less, which may or may not be the case for some geometries when finite element analysis is employed. There are other mathematical methods, however, that can be employed to render field lines, methods that can be much faster than FEA. These methods are not as general as FEA, rather they are specifically suited to certain important and illustrative geometries. We describe here two such geometries which are rich in mathematical and physical insight, and the mathematical techniques which can be used to develop software to quickly render the electromagnetic field in them. In this way we arrive at an effective educational, interactive interface.

The graphics we present here were drawn with such interactive software, developed in the object oriented programming language Agilent Vee Pro. It is not our purpose here to present the specific code developed in this language, but rather the classical mathematical techniques which underlie this code. Most modern graphical languages can be employed to implement these techniques.

2. The parallel plate transmission line.

Probably the most iconic graphic found in Maxwell's plates is that of the parallel plate transmission line. Plate XII in Maxwell's treatise (similar to figure 1) depicts a uniform field deep between the conducting plates, and a fringing field external to the plates, and intense field at the edges of the plates. These fields are due to transverse electromagnetic (TEM) waves propagating on the plates in and out of the screen. In Figure 1 the lines in red (electric field) and the lines in green(magnetic field) divide the cross section into little squares. These lines are everywhere perpendicular, a fundamental fact about guided radiation travelling down the line. Figure 2 shows the transverse electromagnetic

field supported by a slightly different cross section geometry. In any geometry, deep within the plates the lines are uniformly distributed, and the electric field lines terminate uniformly on the conductors, indicating a uniform current distribution. Near the edges, the field lines are much more closely spaced, indicating much greater current density near these edges. Electric field lines also terminate on the external plate faces , indicating a small non uniform distribution of current on these surfaces ,the so called fringing field. The magnetic field lines wrap around the currents in and out of the screen. In figures 1 and 2 only the right side of the symmetric field distribution about the transmission line cross section is shown; there is no need for redundancy. Thus we have a geometry rich in physical insight. Note that in operating the interactive interface to draw figures 1 and 2 the operator is free to specify the plate width and plate separation, and any number of electric and magnetic field lines, in order to form the little squares for any geometry of interest.

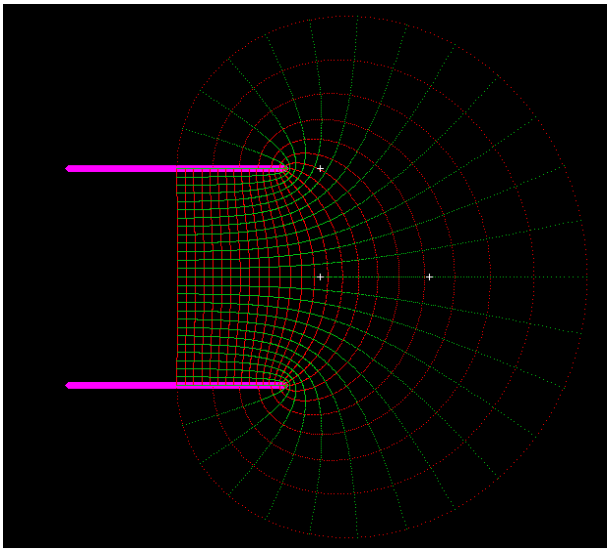

Figure 1

Transmission line cross section for plate separation a=2, and plate width b=2 . Characteristic impedance is 200.6 Ω. The squares form a resistor grid of 26 x 48 = 1248 377 Ω resistors. The white crosses indicate the origin and unit lengths. Any unit of length may be employed.

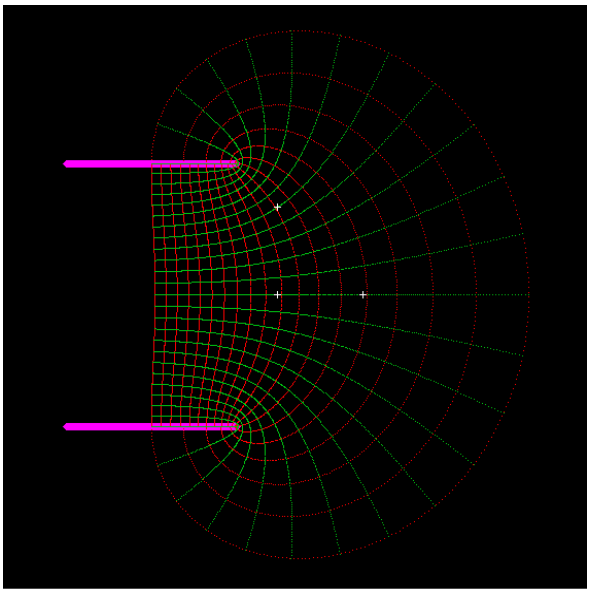

Figure 2

Transmission line cross section for a=3, b=2 Characteristic impedance is 258.7 Ω. The squares form a resistor grid of 24 x 36 = 864 377 Ω resistors.

3. Estimation of impedance.

Transmission line impedance is defined as the ratio of voltage to current of a TEM wave travelling down the line. The voltage and current are given by integrals of the electric and magnetic field, respectively, in a given geometry. Since the field between the plates is nearly uniform, an approximate formula for the impedance of the parallel plate transmission line can be found from these integrals to be

$$377 \ (a/b) \quad \Omega \quad (1)$$

where b is the breadth of the plates and a is the separation, and 377 Ω is the impedance of free space . This formula is accurate only for $a/b << 1$, when the fringing field external to the plates can be neglected.

For many practical lines $b \sim a$, such as in figures 1 and 2, and the fringing field cannot be neglected. It is necessary to find exactly the impedance of such lines.

Historically the impedance of a given cross section was estimated graphically.

As shown in figures 1 and 2, the region of field both internal and external to the line can be accurately divided into many small squares. The squares not deep between the plates are actually square only in the limit of many lines, but their contribution to the impedance can be quantified . The impedance of each square is 377 Ω. These squares can be considered as an array resistors configured in series and parallel. In figure 1, 1248 resistors are configured, 26 in series and 48 in parallel. The impedance of the transmission line is then more accurately given by

$$26/48 \ * 377 = 204.2 \ \Omega \quad (2)$$

Compare this estimate with 377 Ω as found using equation 1. The significant fringing field is in parallel with the uniform field, lowering the line impedance.

In figure 2 the corresponding calculations are

$$24/36 \ *377 = 251.3 \ \Omega$$

Equation 1 in this case predicts 565.5 Ω, meaning the fringing field is actually dominant. The line of figure 2 is of higher impedance than that of figure 1 because the plates are farther apart.

4. Rendering the field lines.

Without the use of a digital computer, the distribution of the squares throughout the cross section has to be established experimentally, for example using conducting silver paint drawn on conducting paper, probed by high impedance voltmeter. In this way the contribution of the fringing field external to the plates is quite accurately accounted for.

To draw the electric and magnetic field lines of figures 1 and 2 more accurately, by computer, the method of conformal mapping is used. Figure 3 shows two complex planes, the xy

plane on the left and the uv plane on the right. The transformation

$$w = a/2\pi * (\exp(z)+z) \qquad (3)$$

maps the rectangular region in xy into the region indicated in uv. Individual line segments forming boundaries in each plane are transformed as shown associated by color. All lines in xy are transformed conformally into uv by this transformation, meaning that angles formed by intersection of lines in xy are preserved upon transformation. It is possible to hypothesize in the rectangle of xy a uniform electromagnetic field. This field will be characterized by straight, uniformly spaced electric and magnetic field lines, mutually perpendicular. Associated with this field is a characteristic impedance. The field lines of the xy rectangle are transformed by (3) into field lines in the uv plane. These are the electric and magnetic field lines drawn in figures 1 and 2.

The impedance of the rectangular geometry in xy is given exactly by (1), specifically

$$377 * (2\pi / (x2-x1)) \qquad \Omega \qquad (4)$$

It is shown in Maxwell (Chapter XII Article 186) that the impedance of the transmission line in uv is exactly equal to that of the line in xy. Thus we have in (4) an exact expression for the impedance of the line in uv, including fringing field, if x2 and x1 are known.

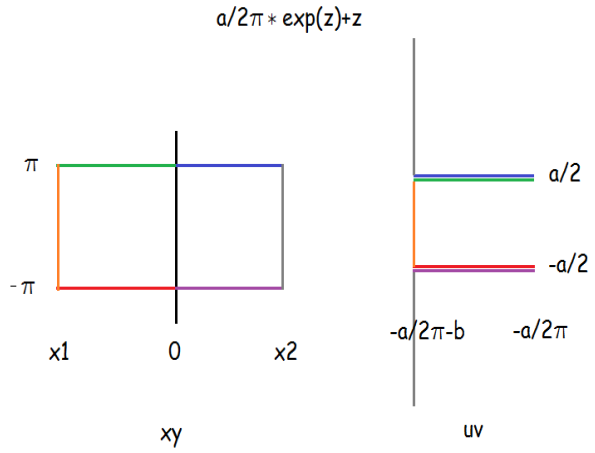

Figure 3

*The conformal transformation a/2 π * exp(z)+z transforms the rectangular region of known impedance on the left into the half plane on the right. The mappings of specific segments are indicated by color. The cross section in uv is of width b and separation a.*

In operation of the interface, the operator specifies the parallel plate geometry in the uv plane. In order to evaluate (4) it is necessary to find by algorithm the magnitudes x1 and x2 in the xy plane that are mapped onto the endpoints of this locus.

Writing out transformation (3) in coordinate form, it is easy to show that two values x1 and x2 satisfy the following equation ,

$$\exp(x)-x = 1+2\pi (b/a) \qquad (5)$$

where the solution x1 is negative and x2 is positive.

This equation cannot be solved in clo sed form. However an iterative algorithm ba sed on Newton's method that quickly converges to x1

and x2 can be coded. With these values, the impedance given by (4) is evaluated for figure 1 and found to be 200.6 Ω. This means the graphical evaluation of impedance was off by about 2 percent. For figure 2 the values x1 and x2 yield impedance 258.7 Ω, an error of about 3 percent.

Once x1 and x2 are known, not only is the impedance exactly known, but it is easy to draw in any language the straight, evenly spaced electromagnetic field lines to cover the xy rectangle for conformal transformation.

The algorithms required in the above considerations, based upon elementary trigonometric and exponential functions, present no particular difficulties in terms of processor speed or memory, so a fast interactive interface can be achieved for this iconic geometry.

5. The Dipole and Conducting Wedge.

As a second example of a two dimensional geometry rich in mathematical and physical insight which can be solved using classical techniques, consider the electrostatic field of a dipole in the presence of a conducting wedge. The dipole, whose electrostatic field in free space is well known, can assume any orientation and position with respect to the conducting wedge. The wedge edge may be of any angle. The dipole will induce surface charge on the wedge. The total field of dipole and wedge is to be rendered, throughout space, for this problem of many degrees of freedom. To render this field graphically we will employ a different conformal transformation, and the classical method of images. Also, a field line drawing algorithm will be needed.

A dipole consists of two equal and opposite charges near one another. If one charge is located at (x1,y1) on the complex plane and its opposite is located at (x2,y2), then the electrostatic potential in two dimensions is of the form

$$\text{Log}(z-(x1,y1)) - \text{Log}(z-(x2,y2)) \qquad (6)$$

where the complex logarithmic potential is used . Figure 4 shows the electric field lines (red) and equipotential surfaces (green) of a dipole in empty space.

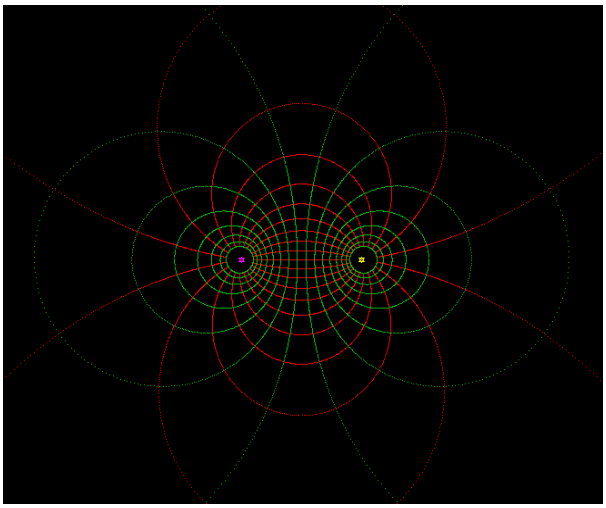

Figure 4

The electric field (red) and equipotential surfaces (green) of a dipole in free space. Note that the lines are everywhere perpendicular, and the field is symmetric.

The algorithm required for drawing the curved lines of figure 4 is more complicated than that employed in the transmission line problem. A field line by definition is at every point aligned in the direction of the local electric field. If the potential under analysis is known, as in (6), then this field can be found at every point as the gradient of the potential. A simple stepping algorithm is then employed to trace out the line. This method can also be used to draw the equipotential surfaces of figure 4, as these lines are at every point perpendicular to the electric field. It is useful to set the step size of the algorithm employed here to be inversely proportional to the local electric field. Under this condition, the points of the lines so stepped will mark off equal potential drops and increments of flux, even in regions of non uniform field. Additionally, the operator is free to adjust the step size depending upon resolution requirements of a particular problem. This is seen in figure 4. The processing time required to find the field lines of figure 4 depends upon the number of red and green lines desired, and the resolution of the stepping algorithms, and can be a few seconds. The number of electric field lines and equipotential surfaces is set so that little squares are formed throughout the cross section, even though this does not have the physical significance (impedance) of the red and green squares of the transmission line problem. This was the style set in Maxwell's plates.

6. The method of images.

In order to introduce the effect of the wedge, we first consider the simpler problem of a dipole near a ground plane, as shown in figure 5. In this problem the dipole induces charge on the ground plane, resulting in field lines terminating perpendicularly on the ground plane. To find an expression for the potential of a dipole near a ground plane, the classical method of images is employed. Given the coordinates of the dipole above the ground plane , introduce

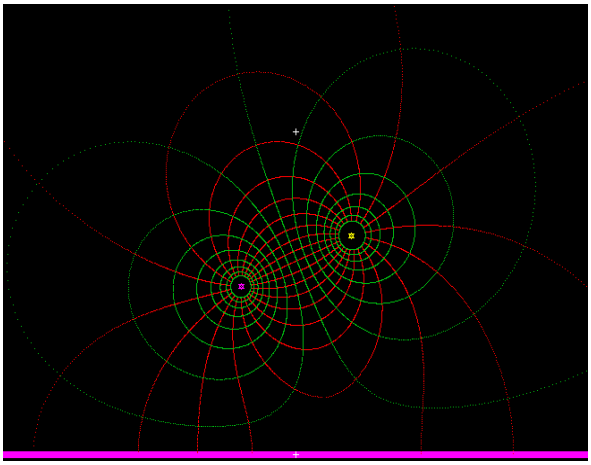

Figure 5

The electric field (red) and equipotential surfaces (green) of a dipole above a conducting ground plane. The field due to induced charge in the ground plane is equivalent to that of an image dipole beneath the plane. Electric field lines are perpendicular to the ground plane.

an image dipole of opposite charges located below the ground plane, spaced symmetrically from the plane. The potential of all four charges is of

$$\text{Log}(z-(x1,y1)) - \text{Log}(z-(x2,y2))$$

$$- \text{Log}(z-(x1,-y1) + \text{Log}(z-(x2,-y2) \qquad (7)$$

The field due to dipole and image has the property that its electric field is at every point of the plane perpendicular to that plane. It therefore solves the boundary value problem of a dipole above a conducting plane; it is the field of the dipole alone above the plane and

the induced charge on the conducting plane. The induced charge density on the plane can be found as the electrostatic flux at the plane. With the potential thus established in (7) by the method of images, the stepping algorithm described above can be applied to render the electrostatic field and equipotential surfaces. As is the case of the parallel plate transmission line, an effective interface will enable the operator to draw any number of field lines, as well as position the charges of the dipole anywhere in space.

7. The conformal transformation z^c

Once the electric field lines and equipotential surfaces above the ground plane are established, a conformal transformation is employed to render field lines in the presence of the wedge. Consider the ground plane in xy (figure 5)to consist of two rays from the origin, left and right. The conformal transformation w = z^c maps these rays into a wedge, and the region above the plane into the region between the conducting wedge faces. If c is between 0 and 1, the transformed region is as shown In figure 6. If c is between 1 and 2, the region is as shown in figure 7. If c is exactly 1, z^c is the identity transformation leaving ground plane unaltered. If c is 2, the ground plane is mapped into a knife edge, as in figure 15.

The transformation z^c is conformal, so it maps the electric field and equipotential surfaces found with the stepping algorithm in figure 5 above the ground plane in xy into mutually perpendicular lines in the presence of the wedge, in uv. These are the desired field lines terminating on dipole and wedge.

In operation of the interface, the operator is free to specify both the wedge angle and the position and orientation of the dipole with respect to the wedge in the uv plane. These degrees of freedom enable the operator to illustrate a wide variety of geometries rich in mathematical and physical insight. Also, the charge density on the wedge faces can be found and charted.

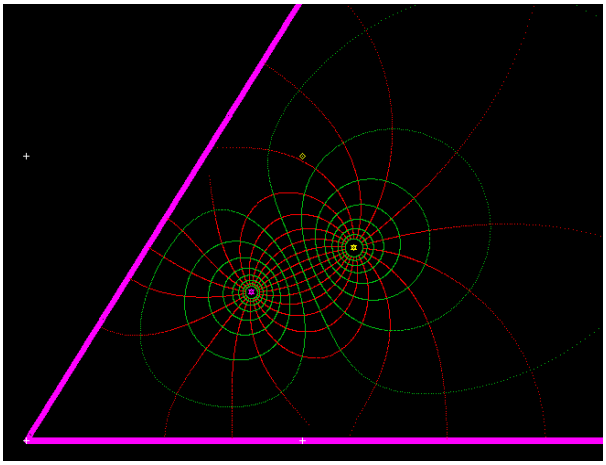

Figure 6

Electrostatic field within a wedge of edge angle 1 radian. Charge is induced on both faces of the wedge. The field is extremely small in the corner of the wedge.

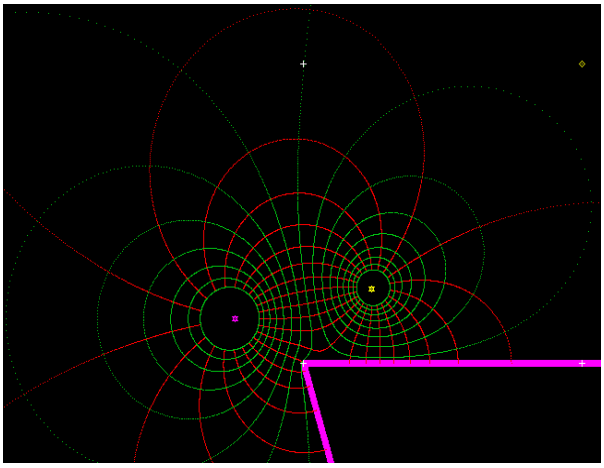

Figure 7

Electrostatic field near a wedge of angle 4 radian. Charge is induced on both faces of the wedge. A large charge density is induced on the wedge corner, attracting electric field lines.

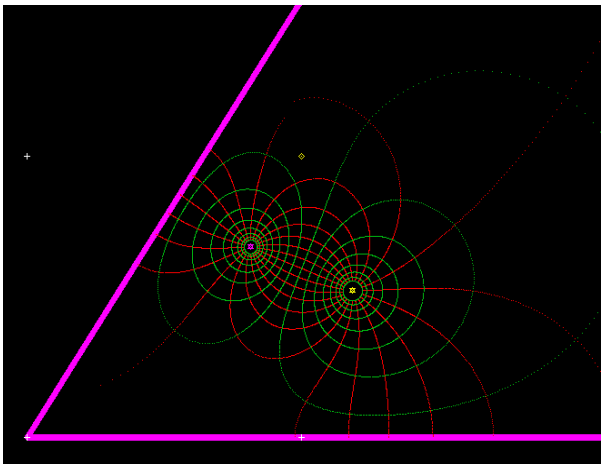

Figure 8

Electrostatic field within a wedge of angle 1 radian. Charge is induced on both faces of the wedge. The field is extremely small in the corner of the wedge.

8. Interpretation of field lines.

In operation of the dipole wedge interface, the operator must, after specifying a geometry, interpret the field lines as presented. As in the case of the parallel plate transmission line, the red electric field lines indicate field intensity by their spacing, the most intense field emerging from and terminating on the charges. A region of fairly uniform field exists between the charges, pointing from charge to charge. The lines terminate or originate on induced charge on the edge faces, if the dipole is positioned near these surfaces. These lines must terminate perpendicularly to the wedge faces. Unlike in the transmission line problem, the green lines of figure 6 are equipotential surfaces. The wedge faces are at ground potential, and the equipotential surfaces are parallel to these faces wherever they are near them. The red and green lines are everywhere perpendicular, a property preserved upon transformation by the conformal mapping z^c. The individual points of the electrostatic field lines , and of the

equipotential surfaces, were drawn in the xy plane to mark equal increments of potential and flux, respectively. These increments are unchanged in the uv plane, another crucial property of the conformal transformation.

9. Surface density and shielding.

The dipole wedge interface can be used to illustrate two important behaviors of electromagnetic fields. Figure 9 shows a plot of the induced surface charge on the wedge faces resulting from the geometry of figure 8. The wedge face aligned along the +u axis is mapped to the right in figure 9, and the oblique face is mapped to the left. This configuration enables a direct examination of the continuity of the induced charge at the wedge edge, at the center of figure 9, which is very important.

The charge induced on the wedge faces depends upon how close to the faces the dipole is, and its orientation. Figure 9 shows the negative charge induced primarily on the left, and the positive charge induced primarily on the right. This is because the dipole of figure 8 is positioned from face to face, slightly closer to the oblique face. In figure 12, positive and negative charge is induced on both faces, because the dipole is rotated to be aligned with a ray from the origin, as in figure 6. In figures 9 and 12 the charge density charted is found numerically as the perpendicular electric flux at the plate surface In the transformed cross section.

In figures 9 and 12 the charge density near the wedge edge is seen to be very small. This is an example of electrostatic shielding, where field is effectively excluded from the corner by induced charge on the wedge faces. This type of shielding is widely employed in electronic equipment design.

Figures 10 and 13 show examples of a dipole positioned near an obtuse wedge. Figures 11 and 14 show respectively the charge induced on the faces, for two dipole orientations. In each case the charge distribution induced on each face follows the dipole. In addition an extremely large charge density appears at the wedge edge. This is shown both by the charted charge density, and by the red electric field lines attracted to the corner. The existence of intense electrostatic field at the sharp corner of a conductor is actually the basis of the lightning rod, as discussed in the references.

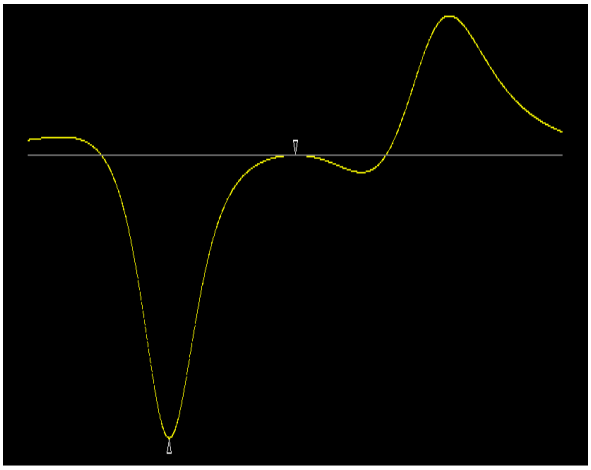

Figure 9

The charge density on the faces of the wedge of figure 8. The wedge corner is indicated by marker in the center. In this region the charge density is extremely small.

The total freedom with which the dipole can be positioned with respect to the wedge enables the interface to illustrate many classical problems. The field of a monopole near a ground plane or wedge can be rendered by positioning the opposite dipole charge far away, so that its influence is negligible. This is done in figure 15, in which a monopole is positioned near a knife edge. It is shown in the references that the charge density near the edge varies as the inverse square root of the

distance to the edge. This distribution is shown by the electric field lines terminating on the knife edge of figure 15. Figure 15 corresponds roughly to plate XI of Maxwell's treatise.

The distribution of charge density near wedge edge is found analytically as a function of wedge angle in several of the references, including by Maxwell using archaic notation. The interface makes it easy to demonstrate these results graphically for any wedge angle, interactively.

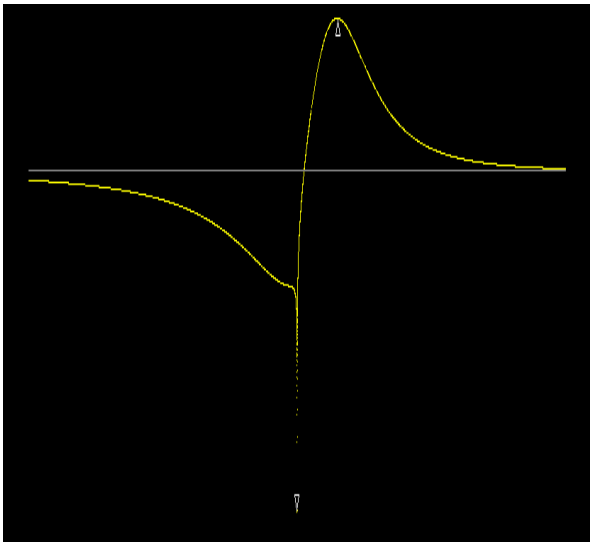

Figure 11

The charge density on the faces of the wedge of figure 10. The wedge corner is indicated by marker in the center. At this point the charge density is extremely large.

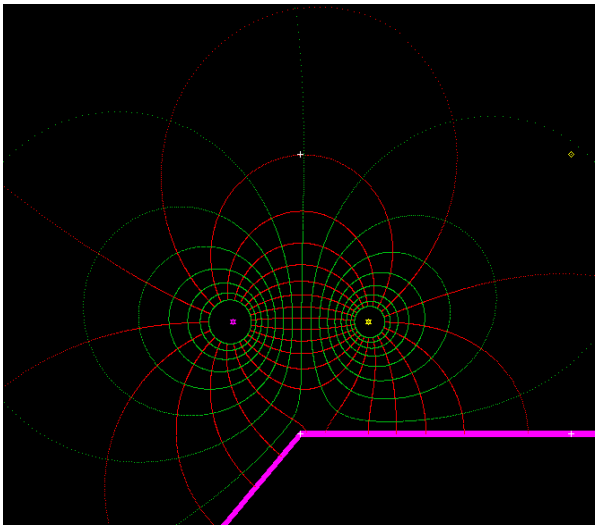

Figure 10

Electrostatic field above a wedge of angle 4 radian. Charge is induced on both faces of the wedge. The charge density is extremely large at the corner.

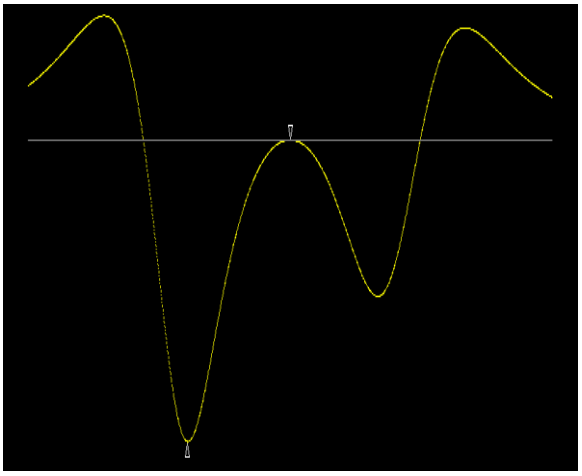

Figure 12

The charge density on the faces of the wedge of figure 6. The wedge corner is indicated by marker in the center. In this region the charge density is extremely small.

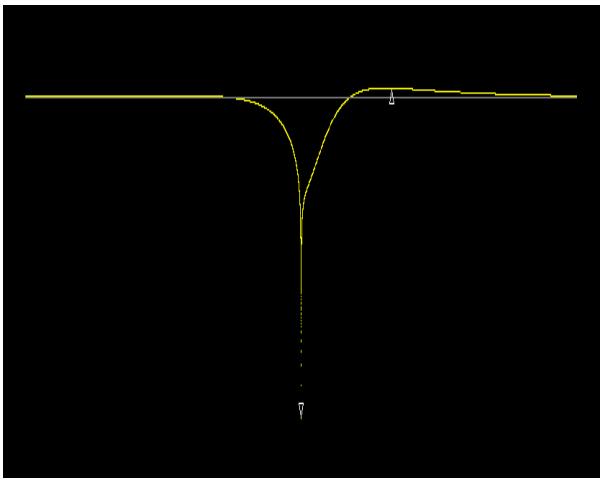

Figure 14

The charge density on the faces of the wedge of figure 13. The wedge corner is indicated by marker in the center. At this point the charge density is extremely large.

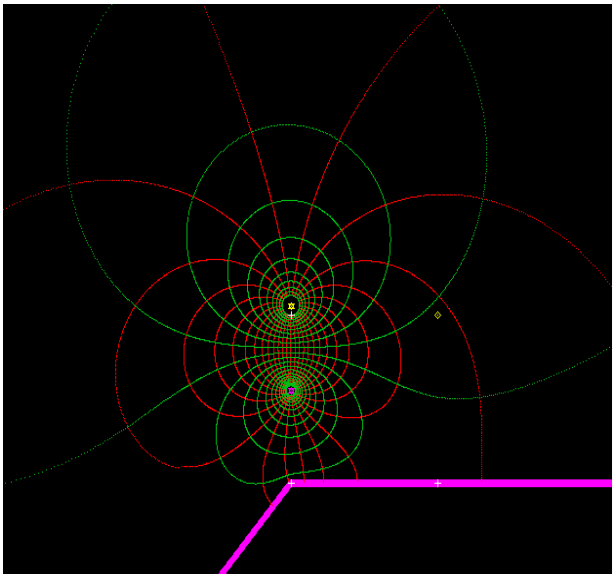

Figure 13

Electrostatic field above a wedge of angle 4 radian. Charge is induced on both faces of the wedge. The charge density is extremely large at the corner.

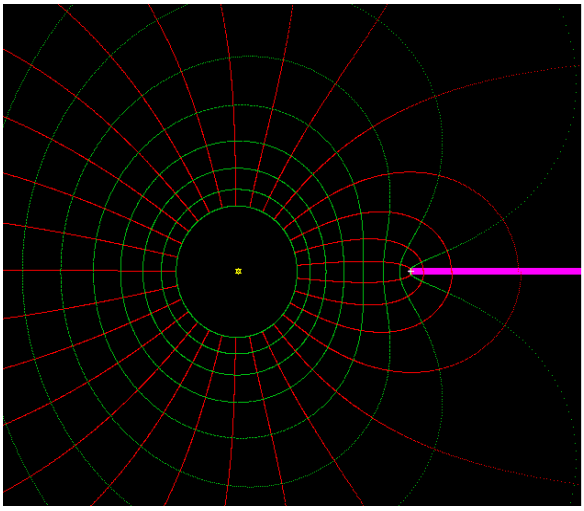

Figure 15

The electrostatic field of a monopole near a knife edge. The other end of the dipole is far enough away to be negligible. The charge density at the knife edge is extremely large. This

graphic corresponds roughly to Plate XI of Maxwell's treatise.

10. Conclusion.

The interactive software described above shows how two electromagnetic field geometries rich in physical and mathematical insight can be rendered effectively using classical techniques and basic algorithms, with existing graphical hardware and software .

There are many more such geometries which can be addressed in this way using other conformal transformations and image techniques. It is possible to foresee the development in the near future of applications on various platforms which will together provide a comprehensive interactive display of many of the properties of the electromagnetic field.

References

Classical Electricity and Magnetism

Panofsky and Phillips 1962

ISBN 0-201-05702-6

Fields and Waves in Communication Electronics

Ramo, Whinnery, Van Duzer

Second Edition 1965

ISBN 0-471-87130-3

Complex Variables and Applications

Ruel V Churchill 1974

Third Edition

ISBN 0-07-010855-2

A Treatise on Electricity and Magnetism

James Clerk Maxwell 1891

Third Edition

486-60636-8

Classical Electrodynamics

John David Jackson 1975

ISBN 0- 471- 43132-X